Comparison of contrast-enhanced ultrasonography and magnetic resonance imaging in evaluating ovarian tumor blood vessels

M. Yang, X. Liu, H. Su*

Department of Ultrasound, Huangshi Maternity & Children's Health Hospital, Edong Healthcare, Huangshi, Hubei, China

▶ *Original article*

ABSTRACT

Background: Our study was to evaluate the value of contrast-enhanced ultrasonography (CEUS) and contrast-enhanced magnetic resonance imaging (CE-MRI) in analyzing the blood vessels associated with ovarian tumors. **Materials and Methods:** A total of 100 patients with ovarian tumors underwent CEUS and CE-MRI before surgery. After surgery, the resected ovarian tissues were evaluated via immunohistochemistry to calculate the tumor microvessel density (MVD), and the correlation between the parameters of CEUS and CE-MRI and MVD in ovarian tumors was determined. **Results:** The MVD level between ovarian tumors was significantly different ($p = 0.03$); the peak intensity (PI) and area under the curve (AUC) of CEUS parameters in malignant tumors were significantly higher than those in benign tumors ($p = 0.03$, $p = 0.03$); and were significantly positively correlated with MVD ($r = 0.57$, $p = 0.00$; $r = 0.50$, $p = 0.00$). The K^{trans} and Ve of CE-MRI parameters in malignant tumors were significantly higher than those in benign tumors ($p = 0.01$ and $p = 0.04$), and were also significantly positively correlated with MVD ($r = 0.66$, $p = 0.00$; $r = 0.55$, $p = 0.00$). Moreover, there was no significant difference between CEUS and CE-MRI in terms of sensitivity (Se), specificity (Sp), negative predictive value (NPV) and positive predictive value (PPV) in malignant ovarian tumors ($p > 0.05$). **Conclusion:** Both CEUS and CE-MRI parameters can reflect the MVD level in ovarian tumors; therefore, CEUS is expected to become a viable alternative approach for evaluating ovarian tumors.

INTRODUCTION

In women, ovarian cancer is the leading cause of death from gynecological malignancies. Microvessel density (MVD) of human tumors is a reliable parameter for evaluating blood vessels associated with tumors [1–3]. Therefore, studying tumor angiogenesis is crucial for tumor treatment and prognosis [4-6]. Imaging means like computed tomography (CT), magnetic resonance imaging (MRI), and Color Doppler Ultrasound have been widely used in the preoperative evaluation of ovarian tumors [7, 8]. Contrast enhanced-MRI (CE-MRI) not only provides morphological signs of tumors, but more importantly, also reflects tumor tissue blood flow, microvascular permeability, vascular permeability, blood vessel density, and even the level of tissue metabolism, among other characteristics [9, 10].

Due to lacking of red blood cell (RBC) reflection and low signal-to-noise ratio, traditional ultrasound has limitations in distinguishing ovarian tumors with relatively small blood vessels and slow blood flow [11-13]. Contrast-enhanced ultrasound (CEUS), however, can evaluate blood flow information by injecting the microbubble contrast agent in the area of interest to quantitatively analyze the blood vessels associated with the tumor. This information can be used to assess the angiogenesis of ovarian tumors prior surgery [13]. To date, few reports have compared CEUS and CE-MRI in evaluating MVD in ovarian tumors.

With the goal of comparing the effectiveness of CEUS and CE-MRI in evaluating MVD in ovarian tumors, the present study analyzed the CEUS and CE-MRI parameters of 100 patients with benign or malignant ovarian tumors, and their relationship with MVD in tumor tissues as detected by immunohistochemistry, with the aim of providing new methods for the diagnosis of ovarian lesions.

MATERIALS AND METHODS

Patient selection

Total of 100 patients with ovarian lesions were included in the present study, and the enrollment period was from 2017 to 2020. The patients ranged from 28 to 76 years, with a median age of 45.8 years. The majority (90/100) were Han Chinese, 4 were Tujia, 3 were Uighur, and 3 were Manchu. Of the 100

patients, 94 were from Hubei province, 2 from Henan province, 2 from Jiangxi province, 1 from Anhui province, and 1 patient was Chinese American. The exclusion criteria were as follows: patients with multiple organ dysfunction, tumors in other parts of the body, metastatic ovarian tumors confirmed by postoperative pathological results, and obvious allergies to contrast agents. All patients performed CEUS and CE-MRI within the three days prior surgery. The present research was authorized by the ethics committee of our hospital (EH20170270S), and written informed consent was obtained from all patients.

Ultrasound examination

In the present study, CEUS was performed using the GE-Voluson E10 ultrasound system (General Electric Company, Fairfield, Connecticut, USA). All exams were performed as follows: (1) routine transvaginal ultrasound and color Doppler measurements of the ovarian mass, echo characteristics, borders, and blood flow distribution; (2) angiography target determination via ultrasound image analysis of ovarian masses; (3) selection of the solid portion of the lesion, the thickness of the cyst wall, the cavity containing the nipple, or the plane with the most blood supply indicated by color Doppler flow imaging (CDFI) [14], and the probe was kept in the same position throughout; (4) Swiss SonoVue (SonoVue, Bracco Suissee SA, Plan-les-Ouates, Switzerland), composed of phospholipid-stabilized shell microbubbles filled with sulfur hexafluoride gas (BR1, Bracco Spa, Milan, Italy) was used as an ultrasound contrast agent. Reagent (25 mg) was mixed with 5 mL 0.9% saline solution, shaken for about 1 min, and then the suspension was manually injected in the anterior cubital vein, immediately after which 5 mL of saline was injected, then the imaging video was recorded. After scanning, the area most significantly enhanced with contrast was selected as the region of interest (ROI) for manually drawing the outline. Quantitative imaging analysis software was used to automatically draw a time intensity curve (TIC) to acquire the parameters during contrast perfusion within the diseased tissue like time of arrival (AT), peak intensity (PI), time to peak intensity (TTP), and area under the curve (AUC).

MRI examination

In the present study, a Siemens Magnetom Trio 3.0T MRI scanner with an 8-channel body phased array coil (Siemens, Erlangen, Germany) was utilized. A 0.1 mmol/kg dose of gadolinium meglumine was injected through the median cubital vein at an injection rate of 2.5 mL/s, using three-dimensional (3D) fast small-angle excitation imaging for multi-period continuous scanning without intervals. The scanning parameters were as follows: repetition time (TR) = 4.1 ms; echo time (TE) = 1.4 ms; layer thickness = 6.0 mm; deflection angle = 14°; and field-of-view (FOV) = 260 × 260 mm. Before the injection, 1–2 period non-enhanced benchmark images were obtained, the same amount of normal saline was injected, and dynamic collection was performed 8 times at an interval of 20 s. To reduce artifacts caused by blood flow and respiration, technologies such as flow compensation, upper and lower pre-saturation, and respiration compensation were used.

Immunohistochemistry

The surgically removed ovarian tumors were stained for CD34 (sc-74499, 1:100; Santa Cruz Biotechnology, Dallas, TX, USA). All staining was performed using a positive control and negative control (phosphate-buffered saline [PBS] instead of the primary antibody). Vascular systems with obvious smooth muscle walls or a lumen with a diameter greater than 8 red blood cells were not counted. A total of five high-vessel density fields were selected for observation to calculate the average MVD value.

Statistical analysis

Quantitative data was expressed as the mean ± standard deviation (SD) and analyzed with GraphPad Prism 7.0 (GraphPad Software, La Jolla, CA, USA). The 2-tailed Student's t test or the Mann-Whitney U test was used to compare the differences between the two groups, and the bi-variate analysis was used to compare the correlation of CE-MRI, CEUS parameters, and MVD of ovarian tumors, and to calculate the r value. The Se, Sp, PPV and NPV of CE-MRI and CEUS in the diagnosis of ovarian tumors were evaluated using the McNemar test.

RESULTS

Postoperative pathology of ovarian tumors and the expression of MVD

Based on the results of the postoperative pathological examinations, patients with ovarian tumors were divided into benign (n=58) and malignant (n=42) groups. The former included 12 serous cystadenomas, 8 serous adenofibromas, 4 mucinous cystadenoma, 12 endometriosis, 12 mature teratomas, 7 fibrotic tumors, 2 corpus luteum cysts, and 1 steroid cell tumors, while the latter included serous papillary carcinomas (n=17), mucinous adenocarcinomas (n=8), endometrioid adenocarcino-mas (n=9), immature teratomas (n=6), a clear cell carcinoma (n=1), and a fibrosarcoma (n=1). Through the immunohistochemical analysis (figure 1), MVD was found to be 37.16±4.35 in benign ovarian tumors, which was significantly lower than that found in in malignant tumors, 39.28±5.39 (p=0.03, table 1).
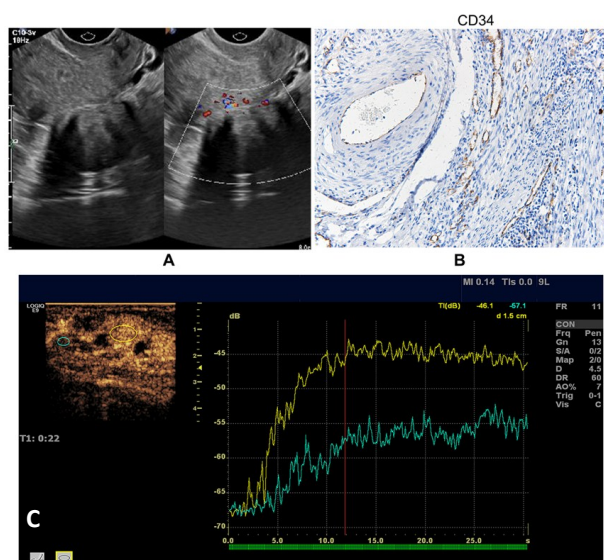
Figure 1. CEUS images and immunohistochemical images of ovarian tumors. **A.** two-dimensional Doppler ultrasound images of ovarian tumors; **B.** CD34 immunohistochemical results of ovarian tumor tissues (×200); **C.** contrast ultrasound TIC of ovarian tumors. CEUS: contrast-enhanced ultrasound; TIC: time-intensity curve.

Table 1. Comparison of MVD levels in ovarian benign and malignant tumors ($\bar{\chi}$ ± SD)

Groups	Benign tumors (n=58)	Malignant tumors (n=42)	t	p
MVD (/HP)	37.16±4.35	39.28±5.39	2.17	0.03

CEUS perfusion parameters in ovarian tumors

As the CEUS data shown in figure 1 and table 2, in the benign tumor lesions, ring-like enhancements could be seen in the cyst wall or nipple of ovarian cysts, while in the malignant tumors, CEUS shows increased overall heterogeneity or rapid dendritic enhancement. PI and AUC in malignant groups were significantly higher than those in benign groups (p=0.03, p=0.03), indicating that the malignant ovarian tumors had abundant blood perfusion.

Correlation between CEUS perfusion and MVD in ovarian tumors

As shown in figure 2, the contrast-enhanced ultrasound perfusion parameters PI (A) and AUC (B) were positively correlated with MVD in ovarian tumors (r=0.57, p=0.00, and r=0.50, p=0.00, respectively).

Table 2. Comparison of ultrasound contrast perfusion parameters in benign and malignant ovarian tumors ($\bar{\chi}$ ± SD).

Groups	AT(s)	TTP(s)	PI (dB)	AUC
Benign tumors (n=58)	15.42±3.31	27.28±7.14	19.15±6.21	18.85±2.89
Malignant tumors (n=42)	13.73±5.20	25.15±8.16	22.50±4.91	21.19±6.12
t	1.85	1.39	2.24	2.30
p	0.07	0.17	0.03	0.03

Figure 2. The correlation between CEUS perfusion parameters and MVD in ovarian tumors. PI: peak intensity; AUC: area under the curve; CEUS: contrast-enhanced ultrasound; MVD: microvessel density.
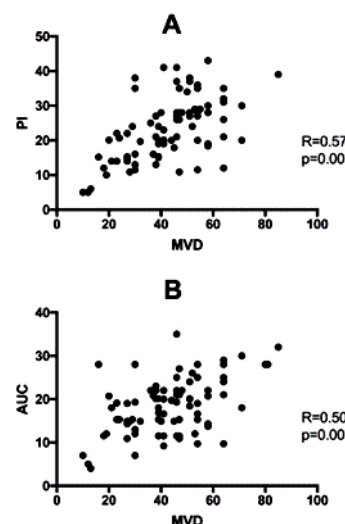
CE-MRI parameters in ovarian tumors

K^{trans} reflects the rate constant of diffusion of the contrast agent from within to the outside of the blood vessel, and is primarily used to reflect the permeability of the blood vessel[15], while Ve represents the size of the extracellular space outside the blood vessel, per unit volume of the tissue. These two parameters are primarily affected by factors such as blood perfusion, MVD, vascular bed permeability, and extracellular space, and have certain significance for observing the vascular microenvironment of ovarian tumor tissue. As shown in table 3 and figure 3, the CE-MRI parameters K^{trans} and Ve were significantly higher in malignant than benign tumors (p=0.01 and p=0.04, respectively).

Table 3. K^{trans} and Ve values in benign and malignant ovarian tumors ($\bar{\chi}$ ± SD).

| Groups	Benign tumors （n=58）	Malignant tumors （n=42）	t	p
K^{trans}	1.25±0.28	1.49±0.51	2.76	0.01
Ve	1.27±0.29	1.68±0.76	2.11	0.04

Correlation between CE-MRI parameters and MVD in ovarian tumors

As shown in figure 4, the CE-MRI parameter K^{trans} (A) in ovarian tumors was positively correlated with MVD (r=0.66, p=0.00), as was the Ve (B)(r=0.55, p=0.00).
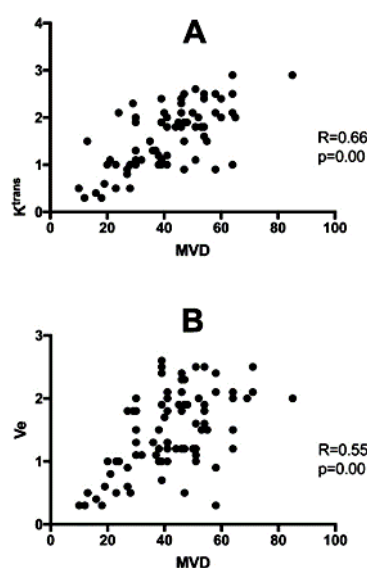
Comparison of CE-MRI and CEUS in the diagnosis of malignant ovarian tumors

As shown in table 4, for 42 malignant ovarian tumors, there was no significant difference between CEUS and CE-MRI in terms of Se, Sp, NPV, PPV, and diagnostic rate (*p*>0.05). CEUS accurately diagnoses 35 malignant ovarian tumors, while 5 cases were misdiagnosed and 7 were missed. CE-MRI, accurately diagnosed 36 malignant ovarian tumors, while 7 cases were misdiagnosed and 6 were missed.
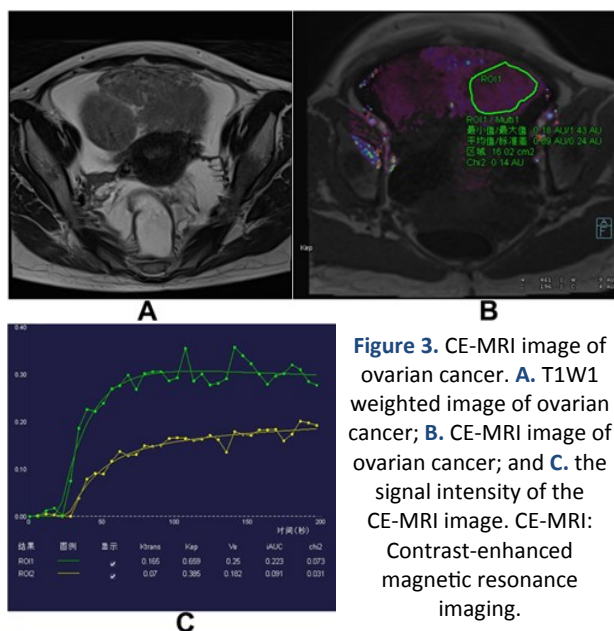
Figure 3. CE-MRI image of ovarian cancer. **A.** T1W1 weighted image of ovarian cancer; **B.** CE-MRI image of ovarian cancer; and **C.** the signal intensity of the CE-MRI image. CE-MRI: Contrast-enhanced magnetic resonance imaging.

Figure 4. The correlation between CE-MRI parameters and MVD in ovarian tumors. CE-MRI: Contrast-enhanced magnetic resonance imaging; MVD: microvessel density.

Table 4. Comparison of CE-MRI and CEUS in the diagnosis of ovarian malignant tumors.

	Se (%)	Sp (%)	PPV (%)	NPV (%)	Diagnostic rate (%)
CEUS	83.3	91.4	87.5	88.3	88.0
CEMRI	85.7	87.9	83.7	89.5	87.0
c2	4.23	1.21	0.14	3.23	3.31
p	0.35	0.22	0.47	0.28	0.15

Se: sensitivity, Sp: specificity, NPV: negative predictive value, PPV: positive predictive value.

DISCUSSION

Among gynecological malignancies, ovarian tumors have the highest mortality rate [16, 17]. Early detection and treatment are key to improving patient survival rates. At present, the clinical diagnosis of ovarian cancer is primarily made through MRI, computed tomography (CT), ultrasound, and other imaging examinations, although in recent years, CE-MRI has become the first choice for assessing the nature of ovarian tumors due to its radiation-free, multi-directional, multi-level imaging, and accurate display of ovarian structure and abnormal disease states [18]. Chase *et al.* [19] used CE-MRI to dynamically observe and evaluate the curative effect of bevacizumab combined with neoadjuvant chemotherapy on breast cancer and anti-tumor angiogenesis, and found that it has good application prospects in the formulation of treatment plans and evaluation of curative effects. In some unusual cases, owing to the presence of an unacceptable implant or device, MRI cannot be performed. Additionally, MRI exams can be quite expensive, which limits its routine application in clinical practice. CEUS has the following advantages: the entire examination is non-invasive, involves no ionizing radiation, has a low cost and repeatable operation, and the method is simpler, especially for repeatability.

The differential diagnosis of gynecological tumors by CEUS is primarily made using three aspects: morphological changes of the vasculature, Doppler signal intensity changes and time intensity curves, and ovarian tumor blood perfusion patterns, which can accurately detect the blood vessels in the tumor [20, 21]. Therefore, CEUS is of great significance for the early diagnosis of malignant ovarian tumors. In the present study, both CEUS perfusion and CE-MRI parameters reflected the expression level of MVD in ovarian tumor tissues. In 2010, Nekkanti *et al.* [22] reported that the ultrasound contrast agent SonoVue was used to distinguish ovarian lesions on vaginal ultrasound examinations, and found that CEUS was more precise in showing microvascular beds than the traditional Doppler imaging, meaning, therefore, that CEUS had a better ability to differentiate the nature of ovarian tumors. Many studies have shown that the prognosis of ovarian cancer is significantly related to tumor angiogenesis [23–25]. Additionally, further comparative data analysis showed that CEUS is similar to CE-MRI in terms of accuracy, specificity, and sensitivity in diagnosing malignant ovarian tumors. According to Fang's [26] research, CEUS, equivalent to CE-MRI, may have an added diagnostic value in human tumors. Therefore, it is expected to become an important method for evaluating ovarian lesions, in addition to CE-MRI.

In conclusion, the CEUS perfusion parameters can be used to assess angiogenesis in ovarian tumors, and are expected to provide non-invasive parametric evidence for the clinical evaluation of ovarian tumor blood vessels in addition to CE-MRI.

contributed the final manuscript.

Conflicts of interest: All authors declare no conflict of interest.

Ethical Approval: The present study was authorized by the ethics committee of Huangshi Maternity & Children's Health Hospital.

Funding: Not applicable.

Author contribution: Mei Yang and Xin Liu performed the experiments and wrote the manuscript, Hongyan Su conceived and designed the analysis, and also reviewed the manuscript.

REFERENCES

1. Guan JH, Cao ZY, Guan B*, et al.* (2021) Effect of Babao Dan on angiogenesis of gastric cancer in vitro by regulating VEGFA/VEGFR2 signaling pathway. *Translational Cancer Research*, **10**: 953-965.
2. Chen XH, Mangala LS, Mooberry L*, et al.* (2019) Identifying and targeting angiogenesis-related microRNAs in ovarian cancer. *Oncogene*, **38**: 6095-6108.
3. Zhang Y, Tang H, Cai J*, et al.* (2011) Ovarian cancer-associated fibroblasts contribute to epithelial ovarian carcinoma metastasis by promoting angiogenesis, lymphangiogenesis and tumor cell invasion. *Cancer Lett*, **303**: 47-55.
4. Kierkels RG, Backes WH, Janssen M*, et al.* (2010) Comparison between perfusion computed tomography and dynamic contrast-enhanced magnetic resonance imaging in rectal cancer. *Int J Radiat Oncol Biol Phys*, **77**: 400-408**.**
5. Ma W, Yang J, Liu N*, et al.* (2020) Are tumor-associated micro-angiogenesis and lymphangiogenesis considered as the novel prognostic factors for patients with Xp11.2 translocation renal cell carcinoma? *BMC Cancer*, **20**.
6. Lin J, Liu ZW, Liao SS*, et al.* (2020) Elevated microRNA-7 inhibits proliferation and tumor angiogenesis and promotes apoptosis of gastric cancer cells via repression of Raf-1. *Cell Cycle*, **19**: 2496-2508.
7. D Fischerová, M Zikán, I Pinkavová*, et al.* (2012) The rational pre-operative diagnosis of ovarian tumors - Imaging techniques and tumor biomarkers (review). *Ceska Gynekol*, **77**: 272-287.
8. Mohaghegh P and Rockall AG (2012) Imaging Strategy for Early Ovarian Cancer: Characterization of Adnexal Masses with Conventional and Advanced Imaging Techniques. *Radiographics*, **32**: 1751-1773.
9. Tuncbilek N, Tokatli F, Altaner S*, et al.* (2012) Prognostic value DCE-MRI parameters in predicting factor disease free survival and overall survival for breast cancer patients. *Eur J Radiol*, **81**: 863-867.
10. Hu LS, Ning S, Eschbacher JM*, et al.* (2015) Multi-parametric MRI and texture analysis to visualize spatial histologic heterogeneity and tumor extent in glioblastoma. *Plos One*, **10**: e0141506.
11. Fang J, Wan YL, Chen CK*, et al.* (2015) Discrimination between Newly Formed and Aged Thrombi Using Empirical Mode Decomposition of Ultrasound B-Scan Image. *Biomed Res Int*, **2015**: 403293.
12. Emilie F, Bruno L and Joël P. (2011) Ultrasound characterization of red blood cells distribution: a wave scattering simulation study. *J Phys Conf Ser*, **269**: 012014.
13. Fleischer AC, Lyshchik A, Andreotti RF*, et al.* (2010) Advances in sonographic detection of ovarian cancer: depiction of tumor neovascularity with microbubbles. *Am J Roentgenol*, **194**: 343-348.
14. Xue W, Yang L, Fan L*, et al.* (2019) Superb microvascular imaging in diagnosis of benign and malignant breast lesions. *Chinese Journal of Medical Imaging Technology*, **1**: 77-81.
15. Meyer HJ, Wienke A and Surov A (2018) Correlation Between Ktrans and Microvessel Density in Different Tumors: A Meta-analysis. *Anticancer Res*, **38**: 2945-2950.
16. Momenimovahed Z, Tiznobaik A, Taheri S*, et al.* (2019) Ovarian cancer in the world: epidemiology and risk factors. *International Journal of Women's Health*, **11**.
17. Umakanthan S, Chattu VK and Kalloo S (2019) Global epidemiology, risk factors, and histological types of ovarian cancers in Trinidad. *J Family Med Prim Care*, **8**: 1058-1064.
18. Xing F and Wu G (2021) Histogram analysis of intravoxel incoherent motion and dynamic contrast-enhanced MRI with the two-compartment exchange model in glioma. *Int J Radiat Res, **19**: 505-514.
19. Dana MC, Michael WS, Bradley JM*, et al.* (2012) Changes in tumor blood flow as measured by Dynamic Contrast-Enhanced Magnetic Resonance Imaging (DCE-MRI) may predict activity of single agent bevacizumab in recurrent epithelial ovarian (EOC) and primary peritoneal cancer (PPC) patients: an exploratory analysis of a Gynecologic Oncology Group Phase II study. *Gynecol Oncol*, **126**: 375-380.
20. Zhou S, Li S, Liu Z*, et al.* (2010) Ultrasound-targeted microbubble destruction mediated herpes simplex virus-thymidine kinase gene treats hepatoma in mice. *J Exp Clin Cancer Res*, **29**: 170.
21. Shen ZY, Hu B, Xia GL, et al. (2014) Ultrasonography of immature teratomas: 11 case reports. *Int J Radiat Res*, **12**: 203-209.
22. Nekkanti R, Nanda NC, Zoghbi GJ*, et al.* (2010) Transesophageal two- and three-dimensional echocardiographic diagnosis of combined left ventricular pseudoaneurysm and ventricular septal rupture. *Echocardiography*, **19**: 345-349.
23. Sopo M, Sallinen H, Hmlinen K*, et al.* (2020) High expression of Tie-2 predicts poor prognosis in primary high grade serous ovarian cancer. *PLoS One*, **15**: e0241484.
24. Alexander K, Sven K, Claudia N*, et al.* (2021) Gene expression in the angiopoietin/TIE axis is altered in peripheral tissue of ovarian cancer patients: A prospective observational study. *Life Sci*, **274**: 119345.
25. Watanabe H, Ichihara E, Kayatani H*, et al.* (2021) VEGFR2 blockade augments the effects of tyrosine kinase inhibitors by inhibiting angiogenesis and oncogenic signaling in oncogene-driven non-small-cell lung cancers. *Cancer Sci*, **112**: 1853-1864.
26. Fang L, Zhu Z, Huang BJ, et al. (2015) A comparative study of contrast enhanced ultrasound and contrast enhanced magnetic resonance imaging for the detection and characterization of hepatic hemangiomas. *Biosci Trends*, **9**:104-110.